



CrossMark
 click for updates

Cite this: *RSC Adv.*, 2016, 6, 40517

Platinum nanopetal-based potassium sensors for acute cell death monitoring†

Irene Taurino,^{‡abc} Solange Massa,^{‡bcd} Gabriella Sanz ,^{ae} Julio Aleman,^{bc} Basilotta Flavia,^a Su Ryon Shin,^{bc} Yu Shrike Zhang,^{bc} Mehmet Remzi Dokmeci,^{bc} Giovanni De Micheli,^a Sandro Carrara^{*a} and Ali Khademhosseini^{‡bcdfg}

Growing interest in the role of ions as cell death regulators has led to the consideration of K^+ , which plays a major role in events such as necrosis, apoptosis and osmotic shock. These mechanisms induce effluxes of K^+ , which can be measured to monitor such cellular events. In this work, we present a fast and simple template-free electrodeposition method for modifying electrodes on microfabricated Si-based platforms with Pt nanopetals. K^+ -selective electrodes were constructed by coupling such newly obtained Pt nanopetals, which were used as a solid contact, with PVC (polyvinyl chloride) K^+ -selective membranes. The drift over time was reduced by three orders of magnitude from several $mV h^{-1}$ for bare electrodes to tens of $\mu V h^{-1}$ when Pt nanopetals were used as an intermediate layer between the electrode and the selective membrane. The improved potential stability is comparable to the best values obtained by using solid-contact ion-selective electrodes based on other nanomaterials. The sensors exhibited near-Nernstian behavior and high selectivity for K^+ . By studying cell viability in relation to K^+ measurements, we established a new correlation between the level of ions and the cell viability upon exposure to both osmotic shock and treatment with acetaminophen. The present method for the continuous and non-invasive monitoring of cell death in a bioreactor has potential applications in various biomedical domains.

Received 19th January 2016
 Accepted 6th April 2016

DOI: 10.1039/c6ra01664b

www.rsc.org/advances

Introduction

The combination of sensing technology¹ and cell-based microfluidic systems has broadened the possibilities of *in vitro* studies,² in particular those investigating cellular events in real time.³ New sensor platforms have been developed to determine cellular functions,⁴ perform drug screening and monitor cell behavior by detecting a wide array of targets ranging from ions to macromolecules.

Potassium is the predominant intracellular ion.⁵ In homeostasis, an intracellular K^+ concentration of around 150 mM is maintained, while its extracellular concentration is 4 mM. The ionic balance is regulated by membrane-bound Na^+/K^+ ATPases, which function by importing K^+ into the cell while exporting Na^+ .⁶ Osmotic shock and necro-apoptotic mechanisms cause disruption of the pump and consequently of the cell membrane, and result in effluxes of K^+ . Fig. 1(a) illustrates a functional Na^+/K^+ pump (left) and effluxes of K^+ resulting from altered Na^+/K^+ pump activity owing to hyperosmotic shock (center) or apoptosis and necrosis (right). Monitoring of K^+ can be used to diagnose cellular dysfunction and, potentially, to predict cell death.⁷

Acetaminophen (APAP) overdose is the primary cause of induced acute liver failure in the United States;⁸ as a consequence, APAP has become the drug of choice for the evaluation of hepatotoxic responses in numerous liver cell lines.⁹ Cell death induced by the use of APAP has been reported to be apoptotic,¹⁰ necrotic¹¹ or necro-apoptotic.¹² In apoptosis, leakage of K^+ creates cell shrinkage¹³ and blebbing accompanied by fragmentation of DNA. Necrosis, on the other hand, results in depletion of ATP, accumulation of reactive oxygen species, and intracellular calcium overload,¹⁴ which causes membrane rupture and the rapid efflux of K^+ . Although the predominant mechanism of cell death during treatment with

^aLaboratory of Integrated System  cole Polytechnique F d rale de Lausanne, 1015 Lausanne, Switzerland. E-mail: sandro.carrara@epfl.ch

^bBiomaterials Innovation Research Center, Division of Biomedical Engineering, Department of Medicine, Brigham and Women's Hospital, Harvard Medical School, Cambridge, MA 02139, USA

^cHarvard-MIT Division of Health Sciences and Technology, Massachusetts Institute of Technology, Cambridge, MA 02139, USA. E-mail: alikh@rics.bwh.harvard.edu

^dPrograma de Doctorado en Biomedicina, Universidad de los Andes, Santiago 7620001, Chile

^eBiosensors Laboratory, Department of Chemistry and Drug Technologies, "Sapienza" University of Rome, 00185 Rome, Italy

^fWyss Institute for Biologically Inspired Engineering, Harvard University, Boston, MA 02115, USA

^gDepartment of Physics, King Abdulaziz University, Jeddah 21569, Saudi Arabia

† Electronic supplementary information (ESI) available. See DOI: 10.1039/c6ra01664b

‡ These authors equally contributed to the work.

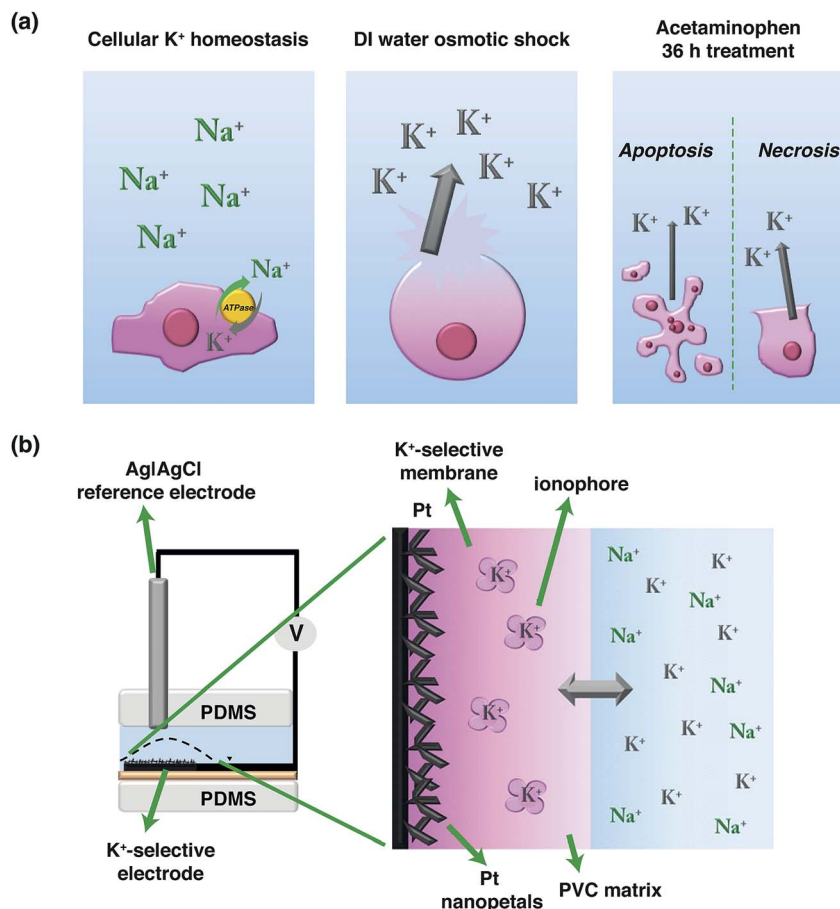


Fig. 1 (a) Unaltered cellular Na^+/K^+ exchange in homeostasis (left) and effluxes of potassium owing to membrane disruption in osmotic shock (center) and apoptosis and necrosis (right). (b) Schematic of the sensor chamber. K^+ ions are captured by ionophores in the ion-selective membrane.

APAP has not yet been established, both possibilities result in the release of K^+ to the extracellular compartment; therefore, the concentration of this ion can be measured to assess cell damage. By inducing acute necro-apoptosis in HepG2/C3A cells, effluxes of K^+ can be measured and then related to the live/dead cell ratio to assess cell viability.¹⁵ The integration of micro-fabricated, stable, and efficient K^+ sensors is therefore useful for monitoring necro-apoptosis in organoids.

Current techniques for estimating K^+ concentrations rely on radiometry,¹⁶ flame photometry, specific electrode photometry, atomic absorption photometry,¹⁷ optical fluorescence (OPTI CCA, Roche Diagnostics) and the patch clamp technique.¹⁸ These methodologies have numerous drawbacks, which include problems with selectivity, off-line detection using large and expensive instrumentation, and repetitive sampling. Potentiometric devices could be used to overcome such problems. In potentiometry, highly selective detection of an ion is achieved by generating a potential difference between a reference and an indicator electrode, the latter being covered with a polymeric membrane that is specifically selective for the ion of interest. The development of fully miniaturized potentiometric cells with long working lifetimes is of key importance for detecting ions in low-volume biological samples. Recently,

solid-contact ion-selective electrodes (SC-ISEs) have been employed to produce small sensing sites with exceptional potential stability and measurement reproducibility.¹⁹ The immediate precursors of SC-ISEs were the so-called coated-wire electrodes (CWEs), in which a selective polymeric membrane directly covered the metal electrode without any intermediate layer. However, they exhibited poor potential stability. To overcome the limitations of CWEs, many electrochemically active layers (solid contacts) have been tested to enable stable and reversible charge transfer between the ionic (selective membrane) and electronic (metal electrode) conductive layers. Conducting polymers have been widely used as intermediate layers in SC-ISEs.^{19e} However, their photosensitivity and the frequent formation of water layers have prompted the development of solid-contact ion-to-electron transducers based on nanostructured materials.²⁰ Nanostructures are not sensitive to light, reversibly convert an ionic signal into an electronic one, and provide high hydrophobicity, which prevents the undesired accumulation of water between the metal electrode and the membrane. The use of gold^{19a} and carbon^{19b} nanomaterials has been extensively investigated for the fabrication of SC-ISEs. Unfortunately, the nanofabrication procedures that have been employed are time-consuming^{19a} or limited to a specific

electrode material.^{19b} Only Skupień *et al.* have used drop-cast Pt nanoparticles as an intermediate layer in ISEs.²¹ On the other hand, nanostructured Pt coatings have been applied as SC-ISEs only in our latest work.²² Other recent studies suggest that nanostructured Pt coatings could be successfully used as solid contacts in reference electrodes.^{19c} However, such coatings have not yet been tested as solid contacts in potentiometric electrodes for measuring electrolytes of biological significance (*e.g.*, K⁺, Na⁺, and Ca²⁺). Furthermore, the use of one-step, template-free, electrodeposited Pt nanostructured layer as solid-contact, ion-to-electron transducer in potentiometry has not been investigated before.

In this work, we report the development of a K⁺-selective electrode based on Pt nanopetals for the continuous monitoring of acute cell death. We produced nanostructured Pt films by a novel and rapid template-free electrodeposition process on a microfabricated Pt electrode of a Si-based sensor. This innovative coating provides stable measurements of K⁺ concentrations over time. In a first stage, the performance characteristics and the measurement reproducibility of the sensor were evaluated with a conventional two-electrode electrochemical cell using a synthetic buffer solution. Then, the sensor was integrated with a microfluidic bioreactor and used to detect K⁺ released by cells (Fig. 1(b)). We determined the effect of deionized water (DI) on HepG2/C3A cells by measuring effluxes of K⁺ due to osmotic shock in real time. We also exposed the cells to treatment with APAP to measure the resulting effluxes of K⁺, and demonstrated the successful use of our novel ion sensor for monitoring necro-apoptotic mechanisms. The novel nano-fabricated sensor functioned at 37 °C in a sterile environment with a bioreactor that was external to the sensor chamber, thus enabling the sensor to measure effluxes of K⁺ at a distance.

Materials and methods

Synthesis of Pt nanopetals

Pt nanopetals were grown using an Autolab PGSTAT101 potentiostat (Metrohm) under computerized control from solutions containing 25 mM H₂PtCl₆ (Sigma-Aldrich) and 50 mM H₂SO₄ (Sigma-Aldrich). Bare electrodes were cleaned before the process by applying a potential of +2 V for 60–120 s. Deposition of Pt was achieved by applying a potential of −1 V for 200 s at room temperature (25 °C) while stirring. A carbon screen-printed electrode (Metrohm), which was used as the counter electrode, was placed in parallel to the indicator electrode to obtain homogeneous depositions. Ag was used as a quasi-reference electrode (Metrohm). After deposition, activation of the material was carried out by acquiring multiple cyclic voltammograms between −0.2 V and +1.5 V at 100 mV s^{−1} in 0.1 M H₂SO₄ until two successive voltammograms overlapped.²³ The cleaning procedure was then repeated.

Ion-selective membrane

A K⁺-selective membrane was obtained by dissolving 32.5% high-molecular-weight poly(vinyl chloride) (PVC, Fluka), 65% bis(2-ethylhexyl) sebacate (DOS, Fluka), 0.5% potassium

tetrakis(4-chlorophenyl)borate (KTClB, Fluka) and 2% potassium ionophore I (Fluka) in 1 mL tetrahydrofuran (THF, Fluka) per 100 mg mixture. Solid-contact K⁺-selective electrodes were obtained by coating Pt nanopetal modified electrodes with 8 μL K⁺ ion-selective membrane and were used as indicator electrodes. The membrane was kept dehydrated for 24 h and then conditioned in 0.01 M KCl (Sigma-Aldrich) overnight before starting the experiments.

Bioreactor design and sensor chamber fabrication

The bioreactor consisted of a glass layer that was permanently plasma-bonded to a polydimethylsiloxane (PDMS) chamber (Sylgard 184, Dow Corning). The PDMS chamber and channels were cast around laser-cut poly(methyl methacrylate) (PMMA) molds that were formerly designed using CorelDRAW® X5 software (Corel Corporation), as previously described.²⁴ After integration of the inlet and outlet 30AWG tubing (Cole-Parmer), the bioreactor was perfused with a 50 μg mL^{−1} solution of type I rat tail collagen (Gibco, Life Technologies) and incubated for 2 h at 37 °C. A total of 20 × 10⁶ HepG2/C3A cells were then seeded in the bioreactor and left to attach for 24 h.

The PDMS sensor chamber was fabricated using laser-cut PMMA molds as described above. After curing the PDMS, the bottom part of the chamber was aligned with the K⁺ sensor before being plasma-bonded to the upper piece. Finally, a central opening was cut in the upper part of the chamber to host the external reference electrode. In the final setup, the medium is drawn from a reservoir by a peristaltic pump, flows successively through the bioreactor and the sensor chamber, and is finally discarded into a waste container while measurements of K⁺ concentrations are recorded.

Pt nanopetal K⁺-selective electrode measurements

The electrochemical characterization of Pt nanopetal K⁺-selective electrodes was carried out in a beaker in a stirred solution (HEPES buffer, pH 5, AppliChem) using a double-junction reference electrode (Metrohm, Ag|AgCl, filling solution: 3 M KCl). The analytical performance of the modified electrodes was studied within the concentration range between 10^{−7} M and 10^{−2} M KCl. Inter- and intra-sample reproducibility was evaluated while stirring at 80 rpm at 25 °C. The effect of stirring on the slope, sensitivity and limit of detection (LOD) was studied. The sensitivity was calculated from the slope of the curve that fitted the data points in the linear range (95% confidence interval according to the IUPAC definition²⁵). The LOD was defined as the K⁺ activity that corresponded to the intersection of the linear regression line and the average potential for K⁺ activities to which the electrode was insensitive.²⁵ The K⁺ activities (*a*_{K⁺}) were correlated to the K⁺ concentrations (*c*) by the extended Debye–Hückel equation.²⁶ The separate solution method was used to calculate the selectivity coefficients.²⁵ In brief, the zero-current potential of the cell was measured in four separate solutions that contained, respectively, K⁺ (0.1 M), Na⁺ (0.1 M), Ca²⁺ (0.1 M) and Mg²⁺ (0.1 M) (three electrodes were tested; stirring at 100 rpm). The selectivity coefficient (*K*_(ion,int)) was calculated from the equation below:

$$\log(K_{(\text{ion},\text{int})}) = ((E_{\text{int}} - E_{\text{ion}})z_{\text{ion}}/(0.059 \text{ V})) + (1 - z_{\text{ion}}/z_{\text{int}})\log(a_{\text{ion}})$$

where z_{ion} and z_{int} are the charges of K^+ and the interfering ion (Na^+ , Ca^{2+} or Mg^{2+}), respectively, and a_{ion} and a_{int} are their respective activities. E_{ion} and E_{int} are the measured average potentials in solutions that contain only K^+ and only Na^+ , Ca^{2+} or Mg^{2+} , respectively. The selectivity coefficient is a number that provides a measure of how well the membrane can discriminate the ion of interest from interfering ions. The lower $K_{(\text{K}^+,\text{int})}$ is, the less the interfering ion affects the measurements. For instance, a value of $K_{(\text{K}^+,\text{Na}^+)}$ of 0.1 means that the electrode is 10 times more responsive to K^+ than to Na^+ . IGOR Pro software (Wavemetrics, OR) was employed for all data analysis. Measurements of biosamples were carried out at flow rates of 16.7 and 9.3 $\mu\text{L min}^{-1}$ using a 600E potentiostat (CH Instruments, Inc.) and a Ag|AgCl reference electrode with a porous Teflon tip (1 M KCl, CH Instruments, Inc.) at 25 °C, or 37 °C when measuring in an incubator. The change in temperature did not significantly affect the slope of the calibration curves. Pt nanopetal K^+ -selective electrodes were calibrated before measuring effluxes of K^+ from the cells in solutions containing 0.05, 0.1, 0.5, 1, 5, and 10 mM K^+ (osmotic shock in distilled (DI) water; resistivity: 18 M Ω cm), or, for concentrations of K^+ in the range between 6 and 16 mM, by steps of 2 mM in the cell medium.

Static DI water exposure and acetaminophen treatment

Cells were seeded at a $1 \times 10^6 \text{ cm}^{-2}$ density in several 96 wells and kept at 37 °C with 5% CO_2 . After 24 h, the plates were exposed to 1, 5, 15 and 30 minutes to DI water while others were subjected to a 36 h treatment with 5, 25 and 50 mM APAP. Medium was removed from each well and the concentration of free K^+ was measured for each treatment. Live and dead assays were immediately performed on all the previous samples.

Cell culture

The HepG2/C3A cell line (ATCC) was cultured at 37 °C with 5% CO_2 in T-175 cell culture flasks. DMEM 1X medium (Gibco) with 10% fetal bovine serum (Gibco) and 1% penicillin-streptomycin (Gibco) was used for culture and replaced every 48 h. Inocula began at a $2 \times 10^6 \text{ cm}^{-2}$ density and cells were harvested at 80% confluency. Cells were counted with a hemocytometer before static and dynamic experiments.

Microscopy and cell viability

Scanning electron microscopy (SEM) images of the nanostructures were acquired with a Zeiss Merlin high-resolution scanning microscope (5 kV), and SEM images of the membrane with a Zeiss Ultra 55 high-resolution scanning microscope (15 kV). Viability images were captured with a Zeiss Axio Observer D1 fluorescence microscope (Carl Zeiss, Germany). A LIVE/DEAD® viability/cytotoxicity Kit (Gibco) was used to assess cell viability under exposure to DI water and treatment with APAP. ImageJ software²⁷ was used for the

quantification of cells and to determine the thickness of the membrane and the dimensions of the Pt nanopetals.

Results and discussion

Fabrication of Pt nanopetal K^+ -selective electrodes

Pt nanopetal-based layers were fabricated by a one-step electrodeposition process as reported elsewhere²² (see Materials and methods section). By this method, electrodes that were homogeneously and fully covered with Pt nanopetals were obtained. The average diameter of the petals was $68 \pm 20 \text{ nm}$. Fig. 2(a) and (b) show SEM images of Pt nanostructures at low and high magnifications, respectively. We deposited Pt nanostructures on the central electrode (geometric area = 7.14 mm^2) of the microfabricated platform highlighted in Fig. 2(c). To fabricate K^+ -selective electrodes, Pt nanopetals were covered with a PVC membrane containing sites selective for K^+ . The membrane exhibited excellent mechanical adhesion to the nanostructured film, which resulted in stable potential readings. The thickness of the membrane, which was calculated from lateral-view SEM images, was $11.7 \pm 2.3 \mu\text{m}$, as shown in Fig. 2(d). After deposition, the membrane was kept dry for at least one day before being conditioned in a solution containing KCl (overnight conditioning). The K^+ concentration in the conditioning solution should be selected to be close to that present in the final sample test. During the conditioning step, K^+ ions enter the membrane. In this way, slow processes of potential equilibration due to changes in K^+ concentrations are prevented. Therefore, a 10 mM KCl solution was chosen, because this concentration was within the range of concentrations of K^+ in cell media. All the steps in the preparation of the Pt nanopetal K^+ -selective electrodes are depicted in detail in Fig. 3.

Sensing performance of Pt nanopetal K^+ -selective electrodes

A potentiometric water layer test was performed to detect the formation of an aqueous layer between the selective membrane

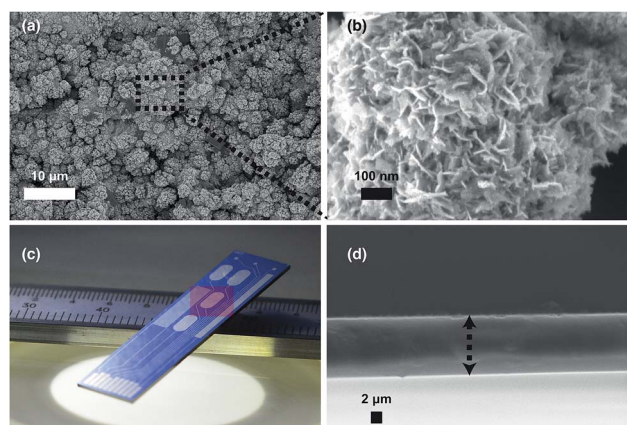


Fig. 2 (a) Low- and (b) high-magnification SEM images of Pt nanopetals. (c) Microfabricated device with the electrode used to construct the Pt nanopetal K^+ -selective electrode in red. (d) Side view of the PVC K^+ -selective membrane. The arrows span the entire thickness of the membrane.

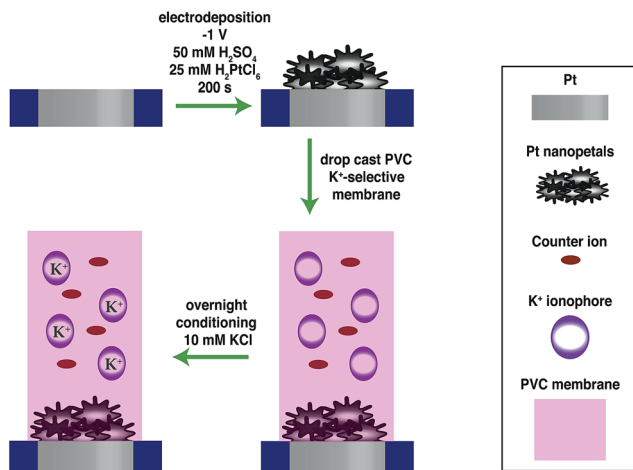


Fig. 3 Construction of Pt nanopetal K^+ -selective electrode.

and the electrode surface, which is the main cause of a long stabilization time following ionic changes in solution.²⁸ For instance, when a K^+ -selective membrane is exposed to a solution of Na^+ , ion-exchange processes cause changes in the ionic composition of the membrane and of the aqueous layer, if one is present. Considering the small volume of the aqueous layer, even small ionic fluxes bring about large variations in concentration that induce large signal drifts (positive if passing from K^+ to Na^+ -containing solutions and negative when the change is in the opposite direction). Measurements were carried out in sequence using the following solutions: 0.1 M KCl, 0.1 M NaCl and 0.01 M KCl. The inset in Fig. 4 shows that drifts occurred when passing from a solution with K^+ to one with Na^+ and *vice versa* only when an electrode without nanostructures was employed. The directions of the two drifts, which are highlighted by arrows, indicate the formation of a water layer when the membrane was cast on bare electrodes. No drift was present when Pt nanopetal-based electrodes were used, which indicates the absence of a water layer between the membrane and the solid contacts.

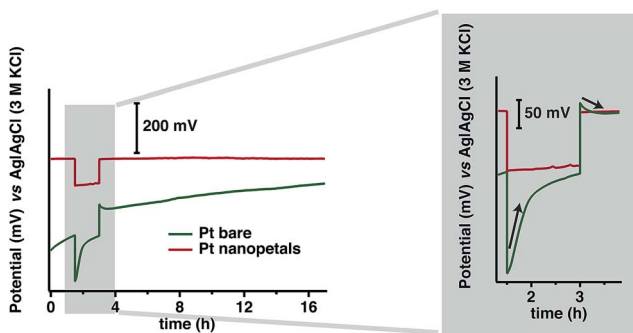


Fig. 4 Water layer test of K^+ -selective electrodes with (red line) and without (green line) Pt nanopetals. The inset highlights positive and negative drifts upon changing the solution from 0.1 M NaCl to 0.1 M KCl and *vice versa*, respectively. Drifts were recorded when bare Pt was used, which indicates that a water layer was present only when Pt nanopetals were not used as a solid contact.

As well as measuring the drift in potential during equilibration processes, it was also established that the mid-term potential stability (Fig. 4) of the electrodes with Pt nanopetals as solid contacts improved by two orders of magnitude compared with that of bare electrodes, as was recently reported by Taurino *et al.*²² These findings were similar to improvements reported in the literature.^{19a,b,21} The lack of adhesion between the two sides of the membrane in the absence of nanostructures is the cause of such high instability when the electrode is used for prolonged intervals.

The sensitivity and LOD were estimated by measuring the open-circuit potential between the Pt nanopetal K^+ -selective electrodes and the reference electrode, and by varying the K^+ concentration in a stirred solution of HEPES. The average sensitivity of four electrodes, which were tested under the same conditions (stirring rate: 80 rpm), was $31 \pm 6 \text{ mV dec}^{-1}$ and the average LOD was $1 \times 10^{(-3.21 \pm 0.07)} \text{ M}$. The same sensor that was tested three times displayed similar values of sensitivity ($30 \pm 5 \text{ mV dec}^{-1}$) and LOD of $1 \times 10^{(-3.18 \pm 0.03)} \text{ M}$.

A sensitivity close to 59 mV dec^{-1} was obtained by stirring the solution at 100 rpm. This result indicates that the electrode potential at equilibrium obeyed the Nernst equation when the K^+ concentration changed. At a stirring rate of above 140 rpm, the linear range increased from 1–10 mM to 0.1–10 mM and the average LOD decreased by one order of magnitude (from approximately $1 \times 10^{-3} \text{ M}$ to $1 \times 10^{-4} \text{ M}$). By increasing the stirring rate from 80 to 170 rpm, the response time fell from a few minutes to seconds. Concentration gradients of K^+ at the membrane-sample interface alter the sensing performance (lower sensitivity, higher LOD and longer response time to ionic changes). Therefore, the minimization of concentration gradients across the membrane during changes in the K^+ concentration in solution is helpful. With this aim, some strategies include the generation of efficient fluxes of ions obtained *via* stirring at a high rate, rotating electrode potentiometry and a high flow rate for measurements under flow conditions.²⁹

Na^+ , Ca^{2+} and Mg^{2+} were considered to be interfering ions because of their presence in all biological fluids. Satisfactory selectivity coefficients were calculated by the separate solution method while stirring (100 rpm), as described in the Materials and methods section. Selectivity coefficients indicate the preference of an electrode for detecting the ion of interest (in our case K^+) over interfering ions (Na^+ , Ca^{2+} and Mg^{2+}). The selectivity coefficients were $\log K_{(K^+,Na^+)} = -2.9 \pm 0.3$, $\log K_{(K^+,Ca^{2+})} = -4.4 \pm 0.5$ and $\log K_{(K^+,Mg^{2+})} = -8.3 \pm 0.1$ ($n = 3$).

Pt nanopetal K^+ -selective electrodes under flow conditions

For the continuous monitoring of cellular effluxes of K^+ , the proposed Pt nanopetal K^+ -selective electrode was inserted in a chamber in line with that containing the cells, and a constant flow was established. Before testing real samples, the modified electrode was characterized under flow conditions. The sensitivity of the electrode was close to Nernstian at a flow rate of $16.7 \mu\text{L min}^{-1}$ and decreased by about 20% when the flow rate was reduced to $9.3 \mu\text{L min}^{-1}$ because of the detrimental effect of a reduced flux of ions, which caused gradients in the K^+

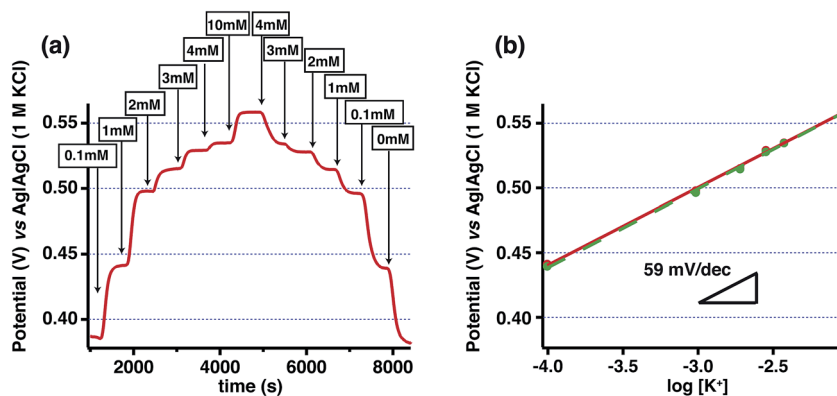


Fig. 5 (a) Measurement of open-circuit potential in HEPES buffer (10 mM, pH 5) recorded for increasing and decreasing concentrations of K⁺ in a flowing system (flow rate: 16.7 $\mu\text{L min}^{-1}$) and (b) the respective calibration curves.

concentration across the membrane (see previous section). Fig. 5(a) shows the change in potential resulting from first an increase and then a decrease in the ion concentration when the device was inserted in a fluidic system. The respective calibration curves are illustrated in Fig. 5(b).

The response of the Pt nanopetal K⁺-selective electrode was still close to Nernstian when DI water and cell media were used as calibration solutions. The aging of the membrane on the Pt nanopetals was also evaluated. The sensor was kept for one week in a conditioning solution (0.01 M KCl) and a decline in sensitivity of 30% was observed with respect to a Nernstian slope. A decrease in the sensitivity of the electrode was observed only when the electrode was stored in the conditioning solution, but aging was absent when the membrane was stored in dry and dark conditions. Indeed, it is well known that a decrease in the response of a sensor is due to prolonged exposure to aqueous solutions that can cause: (1) swelling of the membrane and therefore loss of adhesive strength between the membrane and its substrate;³⁰ and (2) leaching and/or degradation of the ionophore.³¹ On the other hand, an unsuitable (chemically unstable) solid contact would have caused problems with the long-term stability and reproducibility of potential measurements when the sensor was stored in dry conditions. Our novel solid contact based on Pt nanopetals has exhibited an unvarying slope in repeated tests by keeping the sensors dry between tests. This means that Pt nanopetals are excellent solid contacts for K⁺-selective electrodes owing to the absence of detrimental interactions with the K⁺-sensitive polymeric membrane.

Monitoring cell death by osmotic shock

The rupture of cell membranes by osmotic shock is a common lab procedure used to recover the contents of cells, *e.g.*, from yeasts or other microorganisms.^{32,33} Shock by DI water induces cell expansion until the membrane is disrupted and the intracellular contents, including K⁺, flow out into the water. We exposed HepG2/C3A cells to DI water in a 96 well plate and determined the cell viability, as well as the K⁺ concentration, in the water at different time points. With a previously calibrated sensor (S1(a)), we recorded levels of K⁺ after 1, 5, 15 and 30 minutes of exposure to DI water. As

shown in Fig. 6(a), the cell viability started to decrease at minute 1 and an increase in the K⁺ concentration was measured by the Pt nanopetal K⁺-selective electrode. Remarkably, the percentages of live and dead cells correlate well with the measured ion concentrations.

Monitoring cell death by acetaminophen treatment

Acetaminophen (APAP) is one of the most widely used drugs⁸ and is in particular extensively employed in *in vitro* testing.^{9b} Being able to evaluate the effect of treatment with a drug by monitoring cell death *via* direct measurements in the cell medium might be one of the most useful applications of the proposed electrode, when used as a tool to monitor cultured cells. We selected overdose concentrations of APAP reported in the literature³⁴ to evaluate the cytotoxic effects of the drug *via* measurements of K⁺ concentrations. The selected concentrations of APAP caused acute necro-apoptosis in HepG2/C3A cells, and the resulting efflux of K⁺ was measured and compared with the results for live and dead cells. We used 5, 25 and 50 mM APAP in the medium over a period of 36 h in a 96-well plate. After calibrating the electrode in cell media (S1(b)), samples from the wells exhibited a rise in the potentiometric signal, which was in accordance with the live and dead assays (Fig. 6(b)). Treatment with 5 mM APAP did not bring about a significant decrease in viability and therefore the sensor did not respond with an increased signal. On the other hand, 25 and 50 mM APAP caused considerable cell damage even after only 36 h of treatment, and the sensor signal increased as a response to the efflux of K⁺. The proposed novel electrode was able to detect K⁺ for the first time in an undiluted medium under homeostatic conditions, as well as after pharmacological treatments. To the best of our knowledge, this is the first experimental evidence of the possibility of using a potentiometric sensor to quantify the efflux of K⁺ from undiluted cell media during cell culturing. In addition, by measuring the concentration of K⁺ in the medium with our Pt nanopetal K⁺-selective electrode, the percentage of dead cells after treatment with APAP can be calculated. These findings demonstrate the effectiveness and exploitability of the developed K⁺-selective electrode based on Pt nanopetals.

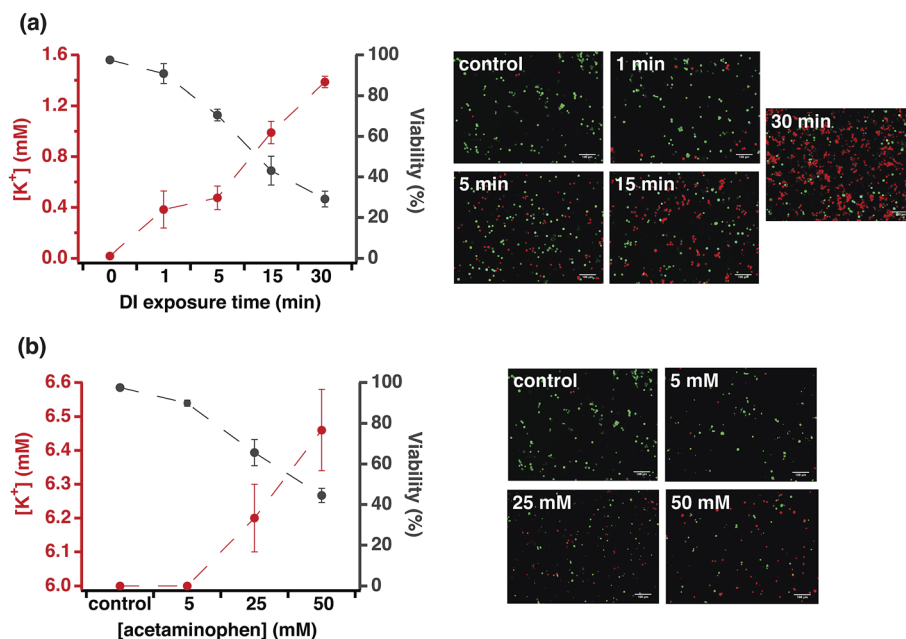


Fig. 6 (a) Measurement of K^+ concentration after 1, 5, 15 and 30 minutes of exposure of cells to DI water. Cell viability was severely decreased after 30 minutes of exposure to DI water (left). Images from a live and dead assay with DI water (right). (b) Increase in K^+ concentration correlated to diminished cell viability after 36 h of exposure to APAP (concentrations: 5, 25, and 50 mM) (left). Images from a live and dead assay for APAP treatment (right).

Continuous monitoring of cell death

Fig. 7(a) shows a schematic of the set-up for continuous monitoring. In brief, a peristaltic pump was connected to a reservoir of medium, which perfused first the bioreactor and then the

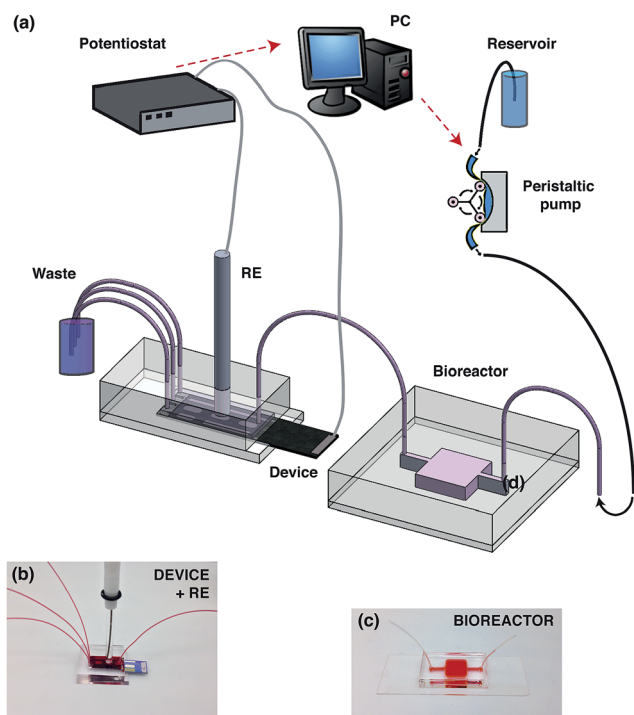


Fig. 7 (a) Schematic of the system for the continuous monitoring of K^+ . Images of the sensor chamber, sensor, and reference electrode (b) and the bioreactor (c).

sensor chamber. Medium or DI water flowed from the sensor chamber into a waste container *via* the outlets. Electrochemical measurements were recorded using a potentiostat connected to both the Pt nanopetal K^+ -selective electrode and the Ag|AgCl reference electrode. Pictures of the sensor chamber and bioreactor are shown in Fig. 7(b) and (c), respectively.

Continuous measurements of the K^+ concentration were carried out by first pumping DI water through the entire system. The potential was stabilized (green line in Fig. 8(a)) prior to connection to the bioreactor. DI water was then introduced into the bioreactor, replacing the medium; the bioreactor was connected to the pump through the inlet and to the sensor chamber through the outlet. With the integration of the bioreactor, the K^+ signal started to increase, which suggested the efflux of K^+ from cells undergoing osmotic shock (red line in Fig. 8(a)). The maximum release of K^+ was obtained after 30 min. The average concentration of K^+ is shown in Fig. 8(b) and corresponds to a cell death rate of about 90%. Following cell exhaustion, the residual K^+ was diluted in a constant flow of DI water during a washing step. In addition, the potential also displayed a trend similar to that reported by others.⁷ Monitoring of cell death *via* the potentiometric quantification of K^+ was previously reported by Generelli *et al.*⁷ However, their experiments were not performed in an incubator and, more importantly, the cells were floating around the sensing site. Here, for the first time, the continuous monitoring of K^+ released by cells in a bioreactor was achieved by using a device hosted in a fluidic chamber that was separate from the bioreactor. The proposed nanopetal-based K^+ -selective electrode can sense K^+ despite the high dilution level that the present set-up

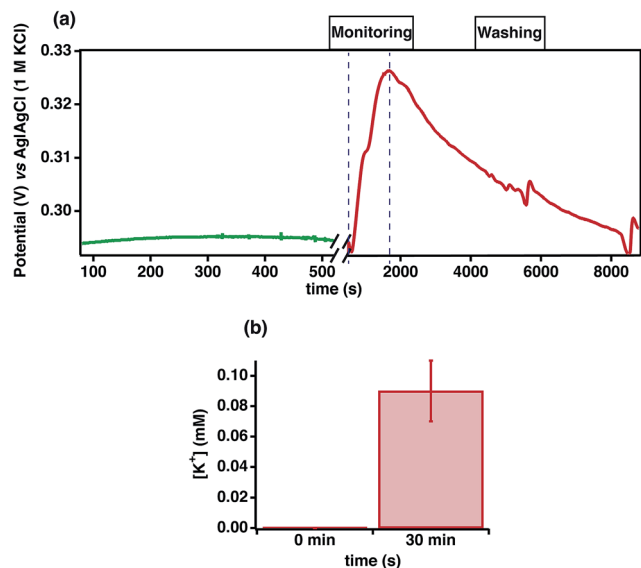


Fig. 8 (a) Stabilization of the potential (green line) prior to connection with the bioreactor. Once the bioreactor was integrated, the sensor signal increased, which indicates the efflux of K^+ from cells ruptured due to osmotic shock (red line). When the cells were exhausted, the remaining K^+ was diluted in a constant flow of DI water in a washing step (red line). (b) K^+ concentration at the starting point and after 30 minutes of exposure to DI water.

entails. In addition, our novel electrode was employed for the first time to monitor the status of a bioreactor directly in sterile conditions at 37 °C. We believe that the latter findings open the possibility of using our Pt nanopetal K^+ -selective electrode for the measurement of K^+ concentrations in biomimetic platforms. The proposed electrodes could also be employed for other applications such as monitoring organ failure (e.g., in intensive care units) or in labs-on-a-chip (e.g., in human organ-on-chip devices).

Conclusion

We fabricated a novel solid-contact K^+ -selective electrode based on electrodeposited Pt nanopetals for measuring the efflux of K^+ from cells as a criterion for the evaluation of acute cell death. Electrodeposited Pt nanostructures have previously been used in potentiometry only to construct pH and reference electrodes.^{19c} In the former studies, the authors employed a template method to produce the film, which is less reproducible and more time-consuming than our nanostructuring protocol.

In our recent work,²² we demonstrated the excellent temporal stability of K^+ -selective electrodes based on Pt nanopetals. In this study, we also demonstrated the excellent sensing performance of the modified electrode, which exhibited near-Nernstian behavior, high reproducibility and selectivity for measuring K^+ concentrations. The suggested sensors exhibited a sufficient LOD for the intended application (monitoring of acute cell death). We also showed that the novel nanopetal-based electrode can be used to quantify acute cell death produced by osmotic shock and necro-apoptosis *via* treatment

with APAP either in DI water or in a regular cell medium. The latter result makes the proposed electrode suitable for bio-samples that already contain K^+ and for events that occur far from the sensing site. The effective performance of the system at 37 °C in a sterile environment enables it to carry out long-term measurements with biological samples.

Potentiometric measurements of K^+ concentrations in cell culture have previously been reported,⁷ but required K^+ -free environments and cells present in the sensor chamber and were not carried out in an incubator. Although there have been previous attempts to construct sensors with electrodeposited nanostructured platinum, this is the first report of the use of such a sensor for a real biological application in the sensing of K^+ ions. In general, our results open the possibility of also using the proposed Pt nanopetal K^+ -selective electrodes to monitor organ and tissue necrosis, which is potentially useful for applications in diagnostics (e.g., intensive care units), as well as for the continuous and critical control of organ-on-chip devices.

Acknowledgements

The EPFL researchers acknowledge funding from the Swiss Confederation. This research was supported by the Project Management Institute Chile (PMI) together with Universidad de los Andes Chile (Programa de Doctorado en Biomedicina). The authors thank Duck-Jin Kim for SEM imaging in Fig. 2(d). The authors also gratefully acknowledge funding by the i-IronIC++ project (Swiss Nano-Tera.ch initiative-Swiss National Science Foundation) and by the Defense Threat Reduction Agency (DTRA) under Space and Naval Warfare Systems Center Pacific (SSC PACIFIC) contract no. N66001-13-C-2027. The authors also acknowledge funding from the Office of Naval Research Young National Investigator Award, the National Institutes of Health (EB012597, AR057837, DE021468, HL099073, R56AI105024), and the Presidential Early Career Award for Scientists and Engineers (PECASE). The publication of this material does not constitute approval by the government of the findings or conclusions herein.

References

- (a) C. Cha, J. Oh, K. Kim, Y. Qiu, M. Joh, S. R. Shin, X. Wang, G. Camci-Unal, K.-t. Wan and R. Liao, Microfluidics-Assisted Fabrication of Gelatin-Silica Core-Shell Microgels for Injectable Tissue Constructs, *Biomacromolecules*, 2014, **15**(1), 283–290; (b) L. Yang, M. Li, Y. Qu, Z. Dong and W. J. Li, Carbon nanotube-sensor-integrated microfluidic platform for real-time chemical concentration detection, *Electrophoresis*, 2009, **30**(18), 3198–3205.
- N. S. Bhise, J. Ribas, V. Manoharan, Y. S. Zhang, A. Polini, S. Massa, M. R. Dokmeci and A. Khademhosseini, Organ-on-a-chip platforms for studying drug delivery systems, *J. Controlled Release*, 2014, **190**, 82–93.
- Y. Shevchenko, G. Camci-Unal, D. F. Cuttica, M. R. Dokmeci, J. Albert and A. Khademhosseini, Surface plasmon resonance fiber sensor for real-time and label-free

- monitoring of cellular behavior, *Biosens. Bioelectron.*, 2014, **56**, 359–367.
- 4 (a) A. Khademhosseini, J. Yeh, S. Jon, G. Eng, K. Y. Suh, J. A. Burdick and R. Langer, Molded polyethylene glycol microstructures for capturing cells within microfluidic channels, *Lab Chip*, 2004, **4**(5), 425–430; (b) H. Y. Hsieh, G. Camci-Unal, T. W. Huang, R. Liao, T. J. Chen, A. Paul, F. G. Tseng and A. Khademhosseini, Gradient static-strain stimulation in a microfluidic chip for 3D cellular alignment, *Lab Chip*, 2014, **14**(3), 482–493; (c) M. De Pinto, D. Francis and L. De Gara, The redox state of the ascorbate-dehydroascorbate pair as a specific sensor of cell division in tobacco BY-2 cells, *Protoplasma*, 1999, **209**(1–2), 90–97; (d) X. Ge, M. Hanson, H. Shen, Y. Kostov, K. A. Brorson, D. D. Frey, A. R. Moreira and G. Rao, Validation of an optical sensor-based high-throughput bioreactor system for mammalian cell culture, *J. Biotechnol.*, 2006, **122**(3), 293–306.
 - 5 F. D. Moore and K. S. Sastry, Intracellular potassium: 40 K as a primordial gene irradiator, *Proc. Natl. Acad. Sci. U. S. A.*, 1982, **79**(11), 3556–3559.
 - 6 S. Genet, R. Costalat and J. Burger, The influence of plasma membrane electrostatic properties on the stability of cell ionic composition, *Biophys. J.*, 2001, **81**(5), 2442–2457.
 - 7 S. Generelli, R. Jacquemart, N. F. de Rooij, M. Jolicoeur, M. Koudelka-Hep and O. T. Guenat, Potentiometric platform for the quantification of cellular potassium efflux, *Lab Chip*, 2008, **8**(7), 1210–1215.
 - 8 H. J. Zimmerman, Drug-induced liver disease, *Drugs*, 1978, **16**(1), 25–45.
 - 9 (a) M. R. McGill, H. M. Yan, A. Ramachandran, G. J. Murray, D. E. Rollins and H. Jaeschke, HepaRG cells: a human model to study mechanisms of acetaminophen hepatotoxicity, *Hepatology*, 2011, **53**(3), 974–982; (b) Y. Dai and A. I. Cederbaum, Cytotoxicity of acetaminophen in human cytochrome P4502E1-transfected HepG2 cells, *J. Pharmacol. Exp. Ther.*, 1995, **273**(3), 1497–1505.
 - 10 I.-S. Park and K. Ja-Eun, Potassium efflux during apoptosis, *J. Biochem. Mol. Biol.*, 2002, **35**(1), 41–46.
 - 11 (a) J. A. Hinson, D. W. Roberts and L. P. James, Mechanisms of acetaminophen-induced liver necrosis, in *Adverse Drug Reactions*, Springer, 2010, pp. 369–405; (b) J. S. Gujral, T. R. Knight, A. Farhood, M. L. Bajt and H. Jaeschke, Mode of cell death after acetaminophen overdose in mice: apoptosis or oncotic necrosis?, *Toxicol. Sci.*, 2002, **67**(2), 322–328.
 - 12 K. Kon, J. S. Kim, H. Jaeschke and J. J. Lemasters, Mitochondrial permeability transition in acetaminophen-induced necrosis and apoptosis of cultured mouse hepatocytes, *Hepatology*, 2004, **40**(5), 1170–1179.
 - 13 C. Bortner and J. Cidlowski, Apoptotic volume decrease and the incredible shrinking cell, *Cell Death Differ.*, 2002, **9**(12), 1307–1310.
 - 14 N. Vanlangenakker, T. V. Berghe, D. V. Krysko, N. Festjens and P. Vandennebeele, Molecular mechanisms and pathophysiology of necrotic cell death, *Curr. Mol. Med.*, 2008, **8**(3), 207–220.
 - 15 C. D. Bortner, F. M. Hughes and J. A. Cidlowski, A primary role for K^+ and Na^+ efflux in the activation of apoptosis, *J. Biol. Chem.*, 1997, **272**(51), 32436–32442.
 - 16 C.-C. Huang, A. C. Hall and P.-H. Lim, Characterisation of three pathways for osmolyte efflux in human erythroleukemia cells, *Life Sci.*, 2007, **81**(9), 732–739.
 - 17 J.-J. Lahet, F. Lenfant, C. Courderot-Masuyer, F. Bouyer, J. Lecordier, A. Bureau, M. Freysz and B. Chaillot, Comparison of three methods for oxidative stress-induced potassium efflux measurement, *Biomed. Pharmacother.*, 2007, **61**(7), 423–426.
 - 18 N. Fertig, R. H. Blick and J. C. Behrends, Whole cell patch clamp recording performed on a planar glass chip, *Biophys. J.*, 2002, **82**(6), 3056–3062.
 - 19 (a) E. Jaworska, M. Wójcik, A. Kisiel, J. Mieczkowski and A. Michalska, Gold nanoparticles solid contact for ion-selective electrodes of highly stable potential readings, *Talanta*, 2011, **85**(4), 1986–1989; (b) J. Ping, Y. Wang, Y. Ying and J. Wu, Application of electrochemically reduced graphene oxide on screen-printed ion-selective electrode, *Anal. Chem.*, 2012, **84**(7), 3473–3479; (c) J. Noh, S. Park, H. Boo, H. C. Kim and T. D. Chung, Nanoporous platinum solid-state reference electrode with layer-by-layer polyelectrolyte junction for pH sensing chip, *Lab Chip*, 2011, **11**(4), 664–671; (d) M. Fibbioli, K. Bandyopadhyay, S.-G. Liu, L. Echegoyen, O. Enger, F. Diederich, P. Bühlmann and E. Pretsch, Redox-active self-assembled monolayers as novel solid contacts for ion-selective electrodes, *Chem. Commun.*, 2000, **5**, 339–340; (e) J. Bobacka, Conducting Polymer-Based Solid-State Ion-Selective Electrodes, *Electroanalysis*, 2006, **18**(1), 7–18.
 - 20 T. Yin and W. Qin, Applications of nanomaterials in potentiometric sensors, *TrAC, Trends Anal. Chem.*, 2013, **51**, 79–86.
 - 21 B. Paczosa-Bator, L. Cabaj, R. Piech and K. Skupień, Platinum nanoparticles intermediate layer in solid-state selective electrodes, *Analyst*, 2012, **137**(22), 5272–5277.
 - 22 I. Taurino, G. Sanz , F. Mazzei, G. Favero, G. De Micheli and S. Carrara, Fast synthesis of platinum nanopetals and nanospheres for highly-sensitive non-enzymatic detection of glucose and selective sensing of ions, *Sci. Rep.*, 2015, **5**, 15277.
 - 23 J. H. Han, S. Park, H. Boo, H. C. Kim, J. Nho and T. D. Chung, Solid-State Reference Electrode Based on Electrodeposited Nanoporous Platinum for Microchip, *Electroanalysis*, 2007, **19**(7–8), 786–792.
 - 24 P. Panda, S. Ali, E. Lo, B. G. Chung, T. A. Hatton, A. Khademhosseini and P. S. Doyle, Stop-flow lithography to generate cell-laden microgel particles, *Lab Chip*, 2008, **8**(7), 1056–1061.
 - 25 R. P. Buck and E. Lindner, Recommendations for nomenclature of ionselective electrodes (IUPAC Recommendations 1994), *Pure Appl. Chem.*, 1994, **66**(12), 2527–2536.
 - 26 A. Craggs, G. Moody and J. Thomas, PVC matrix membrane ion-selective electrodes. Construction and laboratory experiments, *J. Chem. Educ.*, 1974, **51**(8), 541.

- 27 C. A. Schneider, W. S. Rasband and K. W. Eliceiri, NIH Image to ImageJ: 25 years of image analysis, *Nat. Methods*, 2012, **9**(7), 671–675.
- 28 M. Fibbioli, W. E. Morf, M. Badertscher, N. F. de Rooij and E. Pretsch, Potential Drifts of Solid-Contacted Ion-Selective Electrodes Due to Zero-Current Ion Fluxes Through the Sensor Membrane, *Electroanalysis*, 2000, **12**(16), 1286–1292.
- 29 A. Radu, S. Peper, E. Bakker and D. Diamond, Guidelines for Improving the Lower Detection Limit of Ion-Selective Electrodes: A Systematic Approach, *Electroanalysis*, 2007, **19**(2–3), 144–154.
- 30 E. Lindner, V. V. Cosofret, S. Ufer, R. P. Buck, R. P. Kusy, R. B. Ash and H. T. Nagle, Flexible (Kapton-based) microsensor arrays of high stability for cardiovascular applications, *J. Chem. Soc., Faraday Trans.*, 1993, **89**(2), 361–367.
- 31 M. Telting-Diaz and E. Bakker, Effect of lipophilic ion-exchanger leaching on the detection limit of carrier-based ion-selective electrodes, *Anal. Chem.*, 2001, **73**(22), 5582–5589.
- 32 (a) N. G. Nossal and L. A. Heppel, The release of enzymes by osmotic shock from *Escherichia coli* in exponential phase, *J. Biol. Chem.*, 1966, **241**(13), 3055–3062; (b) E. Klipp, B. Nordlander, R. Krüger, P. Gennemark and S. Hohmann, Integrative model of the response of yeast to osmotic shock, *Nat. Biotechnol.*, 2005, **23**(8), 975–982.
- 33 R. Toczyłowska-Mamińska, A. Lewenstam and K. Dołowy, Multielectrode Bisensor System for Time-Resolved Monitoring of Ion Transport Across an Epithelial Cell Layer, *Anal. Chem.*, 2013, **86**(1), 390–394.
- 34 S. J. Fey and K. Wrzesinski, Determination of drug toxicity using 3D spheroids constructed from an immortal human hepatocyte cell line, *Toxicol. Sci.*, 2012, **127**(2), 403–411.